

# RNA Interference Inhibition of Matrix Metalloproteinase-1 Prevents Melanoma Metastasis by Reducing Tumor Collagenase Activity and Angiogenesis

Jessica S. Blackburn,<sup>1</sup> C. Harker Rhodes,<sup>3</sup> Charles I. Coon,<sup>1</sup> and Constance E. Brinckerhoff<sup>1,2</sup>

Departments of <sup>1</sup>Biochemistry and <sup>2</sup>Medicine, Norris Cotton Cancer Center and <sup>3</sup>Department of Pathology, Dartmouth-Hitchcock Medical Center, Lebanon, New Hampshire

## Abstract

**Melanoma incidence is increasing worldwide, and metastatic melanoma is almost completely resistant to every known therapy. New approaches to treating melanoma are urgently needed, and a greater understanding of the biology of melanoma invasion and metastasis will aid in their creation. A high proportion of invasive melanomas have a constitutively active Raf/mitogen-activated protein kinase/extracellular signal-regulated kinase (MEK/ERK) signaling cascade; however, the downstream effectors of ERK signaling that contribute to melanoma invasion and metastasis are unknown. ERK signaling drives the production of the interstitial collagenase matrix metalloproteinase-1 (MMP-1), which is expressed specifically by invasive melanomas. Using short hairpin RNAs (shRNA) to knock down MMP-1 expression in a human melanoma cell line, we investigated the role of MMP-1 in melanoma metastasis in a xenograft model. Knockdown of MMP-1 had no effect on primary tumor growth, but reduction of MMP-1 expression significantly decreased the ability of the melanoma to metastasize from the orthotopic site in the dermis to the lung. Mechanistically, tumor cells expressing MMP-1 shRNAs had diminished collagenase activity, which is required for tumor cell invasion. Additionally, attenuation of MMP-1 expression reduced angiogenesis. These results show, for the first time, that targeted inhibition of MMP-1, a single effector of the Raf/MEK/ERK signaling cascade, prevents the progression of melanoma from a primary to metastatic tumor and, as such, may represent a useful therapeutic tool in controlling this disease.** [Cancer Res 2007;67(22):10849–58]

## Introduction

Melanoma accounts for 4% of all cancer cases, and its incidence is rising at a rate of 3% to 7% per year (1). Progression of melanoma from benign to metastatic tumor is classified histologically, with tumor thickness and depth of invasion being the best prognostic indicators of clinical outcome (1, 2). Early-stage melanoma, classified as radial growth phase (RGP), is confined to the epidermal layer of skin and is readily curable by surgical excision. Later-stage vertical growth phase (VGP) is characterized by invasion of melanoma cells into the dermal layer and is therefore a more serious

disease. VGP frequently progresses into metastatic melanoma, which is almost completely untreatable, and despite decades of research on both cytotoxic and immunologic therapies, the median survival rates of patients with metastatic disease remains only 6 to 9 months (3). The acquisition of an invasive phenotype in melanoma is therefore both clinically and biologically relevant, and work defining the molecular mechanisms of the transition from RGP to VGP is ongoing.

The mitogen-activated protein kinase (MAPK) pathway [Raf/Raf/MAPK/extracellular signal-regulated kinase (ERK)] has been implicated in melanoma progression (4, 5). In particular, the acquisition of constitutively active ERK signaling is linked to the transition of melanoma from RGP to VGP (6, 7). A recent study showed that inhibition of ERK activity prevents the growth of melanoma lung metastases (8), indicating that genes acting downstream of ERK are important in melanoma metastasis. However, ERK has >50 substrates and induces the expression of several genes involved in melanoma progression (9). The exact mechanism by which ERK signaling facilitates the transition from RGP to invasive VGP and its contribution to melanoma metastasis is therefore unknown.

We and others have shown that ERK signaling in melanoma induces expression of the interstitial collagenase matrix metalloproteinase (MMP)-1 (10, 11). MMPs are a family of at least 23 enzymes that are secreted by cells and cleave the protein components of the extracellular matrix (ECM), such as collagen, fibronectin, and laminin, and also proteolytically activate non-matrix substrates, such as growth factors and cell surface receptors (12, 13). In normal tissue, MMP expression is tightly regulated, but in many cancers, including melanoma, MMPs are overexpressed by both the tumor and surrounding stromal cells. This up-regulation of MMPs is linked to many aspects of cancer progression, including tumor growth, invasion, and metastasis and tumor-induced angiogenesis (14, 15).

In melanoma, proteolysis of the basement membrane between the epidermal and dermal layers, and degradation of the ECM within the dermis, is essential for tumor invasion and metastasis. In many cancers, this proteolytic degradation of the ECM is mediated by MMPs (16). Melanoma expresses several different MMPs, and their expression pattern changes throughout the different stages of melanoma progression (17, 18), with MMP-2, which degrades the type IV collagen of basement membrane, being frequently linked to an invasive phenotype (19, 20). MMP-1 has not been well studied in melanoma progression, although its primary substrate, type I collagen, is a major component of the dermal layer of skin, and MMP-1 expression is necessary for melanoma cell invasion through synthetic ECMs *in vitro* (21–23).

To define the role of MMP-1 in melanoma progression, we knocked down MMP-1 expression in the VMM12 human metastatic

**Note:** Supplementary data for this article are available at Cancer Research Online (<http://cancerres.aacrjournals.org/>).

**Requests for reprints:** Constance E. Brinckerhoff, Department of Medicine, Dartmouth Medical School, 1 Medical Center Drive, Lebanon, NH 03756. E-mail: [brinckerhoff@dartmouth.edu](mailto:brinckerhoff@dartmouth.edu).

©2007 American Association for Cancer Research.  
doi:10.1158/0008-5472.CAN-07-1791

melanoma cell line using short hairpin RNAs (shRNA). VMM12 cells are an aggressive line with constitutively active ERK signaling and thus express high levels of MMP-1 (10). Here, we show that although the targeted knockdown of MMP-1 did not affect primary tumor growth, it significantly inhibited the overall collagenase activity of the tumors and prevented melanoma metastasis. Further, expression of MMP-1 shRNAs blocked tumor-induced angiogenesis, which likely contributed to the decreased metastatic potential of the tumors. Together, these results show that MMP-1, a single downstream effector of ERK signaling, is an important mediator of melanoma metastasis.

## Materials and Methods

**Cell lines.** The VMM12 human melanoma cell line was cultured as described previously (10). For serum-free conditions, cells were cultured in DMEM supplemented with 0.2% lactalbumin hydrolysate. Human microvessel endothelial cells (HMVEC; Cascade Biologics) were cultured on dishes coated with attachment factor (Cascade Biologics) in medium 131 containing microvascular growth supplement (Complete Media, Cascade Biologics).

**shRNA expression plasmids.** We have described the creation of a shRNA expression plasmid previously (24). In the present study, three different MMP-1 shRNA oligonucleotides (sh5', sh305, and sh3') were cloned into the pSuper-retro-puro expression vector (OligoEngine). Each oligonucleotide contained a region specific to MMP-1 mRNA, a hairpin loop region, and 5' and 3' linker sequence. The regions specific to MMP-1 mRNA for each oligonucleotide were as follows: 5'-GGAAGCCATCACTTACCTTGC-3' corresponding to bases 26 to 46 of the MMP-1 mRNA (sh5'), 5'-ACCAAG-ATGCTGAAACCTG-3' corresponding to bases 305 to 323 of the MMP-1 mRNA (sh305), and 5'-GCAAGGATAACTCTTCTAAC-3' corresponding to bases 1900 to 1920 of the mRNA (sh3'). The sequence for sh305 has been described (24) and the sh5' and sh3' sequences were designed using the Block-iT shRNA design algorithm (Invitrogen). A mammalian scrambled oligonucleotide (MAMM-X; OligoEngine), not homologous to any known mammalian sequence, was ligated into the pSuper-retro-puro vector as a shRNA control (shMAMMX).

**Generation of stable cell lines.** VMM12 cells were transfected with each of the shRNA plasmids using Lipofectamine 2000 (Invitrogen) following the manufacturer's protocol. Stable cell lines were selected with 1.5  $\mu\text{g}/\text{mL}$  puromycin (Calbiochem), and individual clones were isolated using cloning discs (PGC Scientific). Total cellular RNA was harvested using the RNeasy RNA isolation kit (Qiagen), and MMP-1 mRNA was measured using real-time reverse transcription-PCR (RT-PCR; see below). Four clones from each of the sh5', sh305, and sh3' groups were chosen based on >80% knockdown of MMP-1 mRNA levels compared with the parental VMM12 line, and four clones were selected from the shMAMMX group that had MMP-1 mRNA expression equal to that of the VMM12 cells. Clones from each group were maintained separately and then pooled immediately before experiments.

**Real-time RT-PCR.** Reverse transcription of total cellular RNA was done using the Taqman Reverse Transcription reagent kit (Applied Biosystems) following the manufacturer's directions. Real-time PCR was done using Syber Green master mix (Applied Biosystems) as described previously (24). All assays were done in triplicate, with machine duplicates, and a plasmid-based standard curve was included to quantitate the mRNA of interest. Data are presented as average number of copies of MMP per copy of  $\beta$ 2-microglobulin ( $\beta$ 2M) for three or more individual experiments. Primers used in these analyses are listed in Supplementary Table S1.

**MMP-1 ELISA.** Clones from each cell line were pooled and plated at a density of  $5 \times 10^5$  cells per well in six-well plates. Cells were cultured in serum-free DMEM for 24 h and 100  $\mu\text{L}$  of the medium were used in the human MMP-1 Biotrak ELISA system (Amersham) according to the manufacturer's directions. Nanograms of MMP-1 protein from the ELISA were normalized to micrograms of total protein and assays were done in triplicate, three individual times.

**In vitro collagen degradation assay.** Bovine type I collagen (Organogenesis) was buffered as described (25), with the addition of 10  $\mu\text{g}/\text{mL}$  trypsin, which is required to activate the latent MMPs secreted by the VMM12 cells. Pooled clones from each cell line ( $2.5 \times 10^5$  total cells) were mixed with 1 mL collagen and plated into one well of a six-well plate. Collagen was allowed to gel, and 1 mL of serum-free DMEM was added to each well. After 72 h at 37°C, the media were collected from each well and weighed. The weight of the medium added at the start of the assay (1 g) was subtracted from the total amount of medium in the well at the end of the assay to quantify the liquid liberated from the gel due to collagen degradation. Side-view photographs of the plates were taken, and data are presented as the average weight of medium in excess of 1 g for three individual experiments, done in triplicate.

**Orthotopic injection into nude mice.** On the day of injection, cells from each shRNA clone were counted using a hemocytometer. Equal numbers of cells from each clone were pooled, and a total of  $5 \times 10^6$  cells from each of the VMM12 parental, shMAMMX, sh5', sh305, and sh3' groups was resuspended in 500  $\mu\text{L}$  HBSS. Cells ( $5 \times 10^5$ , 50  $\mu\text{L}$ ) were injected interdermally into the right flank of 6-week-old female nude mice (strain *nu/nu*; Charles River). Seven mice were injected with each cell line. Tumor diameter was recorded weekly; mice were sacrificed when tumors reached 12 mm in diameter. Animal studies were approved by the Institutional Animal Care and Use Committee at Dartmouth College.

**PCR analysis of lung metastases.** To quantitate human DNA in mouse lung, the left lung from each mouse was removed at dissection and DNA was extracted from the tissue using the Puregene Tissue Core Kit A (Qiagen) following the manufacturer's directions. Real-time PCR to amplify a repetitive human *AluI* sequence was done on 100 ng of lung DNA using Syber Green master mix and the primers 5'-CGAGCGGGTGGATCATGAGGT-3' (forward) and 5'-TCTGTGCGCCAGGCCGGACT-3' (reverse) as described previously (26). A standard curve, made by combining a serial log dilution of human DNA (Promega), ranging from 100 ng to 1 pg, with 100 ng murine DNA (Promega), was included with each assay to quantitate the amount of human DNA in each lung sample. Data are presented as the log of pg human DNA per 100 ng lung DNA; each data point represents the average of three separate PCRs on the lung tissue of one mouse.

**Tissue staining.** A cross-section of tumor and right lung was collected from each mouse at dissection and fixed in 10% paraformaldehyde. Tissues were paraffin embedded, sectioned, and stained with H&E to visualize lung metastases, with Masson's trichrome to highlight blood vessels, and for murine CD31 antigen (Abcam) and human MMP-1 antigen (Calbiochem). Staining was done by the Department of Research Pathology, Dartmouth-Hitchcock Medical Center. Micrographs were taken using an Olympus IX50 inverted microscope, equipped with a QImaging digital camera, and QCapture Pro software. Lung metastases were counted on three H&E-stained lung sections from each mouse, and the number was normalized to the area of lung tissue on the slide. To measure the size of lung metastases, micrographs of the seven metastases found in the H&E-stained lung sections of MMP-1 shRNA-injected mice were taken at  $\times 10$  magnification. Micrographs were also taken of seven randomly chosen lung metastases of VMM12- and shMAMMX-injected mice, and QCapture Pro software was used to measure the longest width and height of each of the metastases. Area was calculated using  $(\pi / 4)(\text{length} \times \text{height})$ . Data are the  $\log_{10}(\text{area of metastasis})$ . The microvessel density of each tumor section was found by counting the number of CD31-positive vessels per field, at  $\times 20$  magnification, for three random fields. Data are the average number of blood vessels per field. To measure luminal width, micrographs were taken of three random fields per slide at  $\times 10$  magnification, and QCapture Pro software was used to measure the smallest width of the luminal space within each vessel. Results are the average width in  $\mu\text{m} \pm \text{SD}$  of vessels per field.

**Collagenase activity of tumor explants.** A cross-section of each tumor was weighed and placed in a 24-well dish containing 1 mL serum-free DMEM per well. At 24 h, media were collected and type I collagenase activity was measured using the Collagenase Activity Assay kit (Chondrex) following the manufacturer's protocol. In some experiments, 1  $\mu\text{g}/\text{mL}$  anti-FLAG or 1  $\mu\text{g}/\text{mL}$  anti-MMP-1 neutralizing antibody (Chemicon) was added

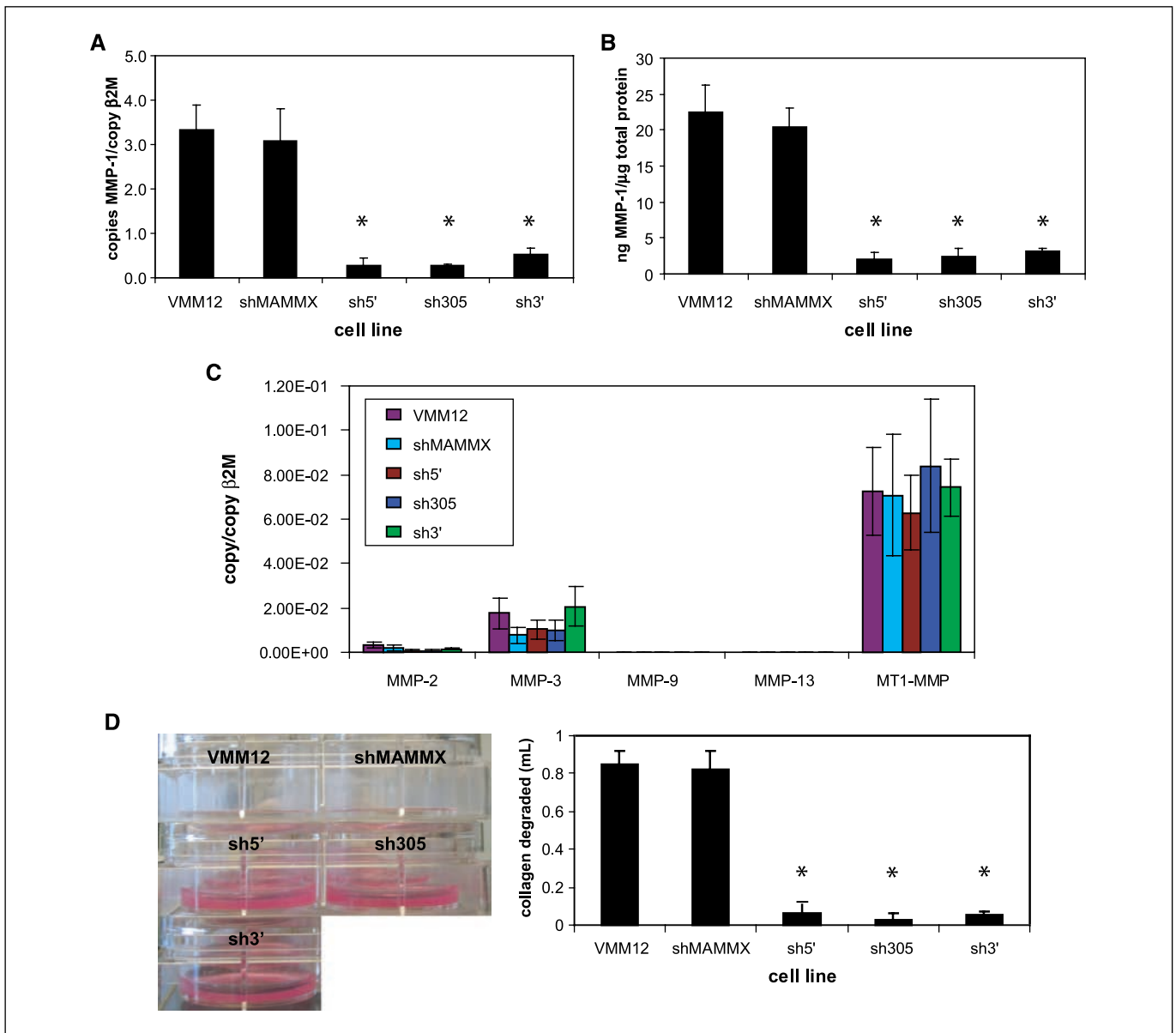


**Figure 1.** MMP-1 shRNAs selectively inhibit MMP-1 expression and activity in VMM12 melanoma cells. **A**, real-time RT-PCR quantification of the MMP-1 mRNA levels of each cell line showed that the three MMP-1 shRNA cell lines have MMP-1 mRNA expression knocked down by at least 80% compared with the VMM12 cells. shMAMMX shRNA has no effect on MMP-1 expression. **B**, MMP-1 shRNAs also block MMP-1 protein production as measured by MMP-1 ELISA. **C**, shRNA expression did not affect the expression of other MMPs as measured by real-time RT-PCR quantification of MMP-2, MMP-3, MMP-9, MMP-13, and MT1-MMP mRNA levels. **D**, MMP-1 shRNAs significantly inhibit MMP-1 activity as measured by an *in vitro* collagen destruction assay. Cell lines were embedded in collagen as described in Materials and Methods. After 96 h, the media were removed from each well, and the remaining collagen gel was photographed. The medium removed from the wells was weighed to quantitate the extent of collagen degradation. **C** and **D**, columns, mean of three individual experiments done in triplicate; bars, SD. \*,  $P < 0.001$ , compared with shMAMMX control.

to explant conditioned medium before use in the assay. The fluorescence intensity of the supernatants was measured at a 520-nm emission wavelength and a 490-nm excitation wavelength using a SpectraMax M2 spectrophotometer. The collagenase activity of each explant was calculated using the formula provided with the assay kit and normalized to the weight of the explant. Data are the mean  $\pm$  SD collagenase activity of explant groups measured in two individual assays.

**Tube formation assay.** For conditioned medium, clones from each melanoma cell line were pooled and plated at a density of  $5 \times 10^5$  cells per well in a six-well plate. After 24 h, 1 mL basal medium, consisting of medium 132 (Cascade Biologics) supplemented with 2% fetal bovine serum, was added to each well and conditioned for 48 h. In the tube formation

assay, 50  $\mu$ L of growth factor-reduced Matrigel (BD Biosciences) were plated into each well of a 96-well plate and allowed to solidify, and then  $5 \times 10^3$  HMVECs resuspended in 100  $\mu$ L of conditioned medium were added into each well. For experiments using neutralizing antibody, either 1  $\mu$ g/mL of neutralizing MMP-1 antibody (Chemicon) or 1  $\mu$ g/mL FLAG antibody (Sigma) was added to the shMAMMX conditioned medium immediately before HMVECs were added to the medium. For experiments using protease-activated receptor-1 (PAR-1) inhibitor, HMVECs were pretreated with 25  $\mu$ mol/L SCH79797 (Tocris) or an equal  $\mu$ L amount of DMSO for 15 min before addition to the shMAMMX conditioned medium. Cells were incubated at 37°C for 72 h. Micrographs were taken using an Olympus IX50 inverted microscope, equipped with a QImaging digital camera. The data

are the average of number of branch points per well and are representative of four individual experiments done in triplicate.

**Statistical analyses.** Statistical analyses were done using JMP statistical software, version 5.01. Linear contrasts in one-way ANOVA were used to calculate the statistical significance for all experiments, except for the quantification of H&E-stained lung metastases, for which a Welch ANOVA test was used. Statistical significance was assigned to  $P$  values of  $\leq 0.05$  and is indicated with asterisks (\*) in the figures.

## Results

**Stable expression of MMP-1 shRNAs specifically knocks down MMP-1 expression and activity in VMM12 melanoma cells.** Human VMM12 melanoma cells express high levels of

MMP-1 due to activated ERK signaling (10) and are aggressively growing and metastatic when injected orthotopically into nude mice (Supplementary Fig. S1). To examine the role of MMP-1 in melanoma growth and metastasis, MMP-1 expression was stably knocked down in VMM12 cells using shRNAs. The three resultant lines, named sh5', sh305, and sh3', had at least an 80% knockdown of MMP-1 expression compared with parental VMM12 cells, whereas the control shRNA cell line, shMAMMX, had no change in MMP-1 expression as measured by mRNA (Fig. 1A) and protein (Fig. 1B) levels. Additionally, the shRNAs caused no change in the expression of other MMPs that are frequently linked to tumor progression (16), specifically MMP-2, MMP-3, MMP-9, MMP-13, and membrane type 1-MMP (MT1-MMP; Fig. 1C). These results

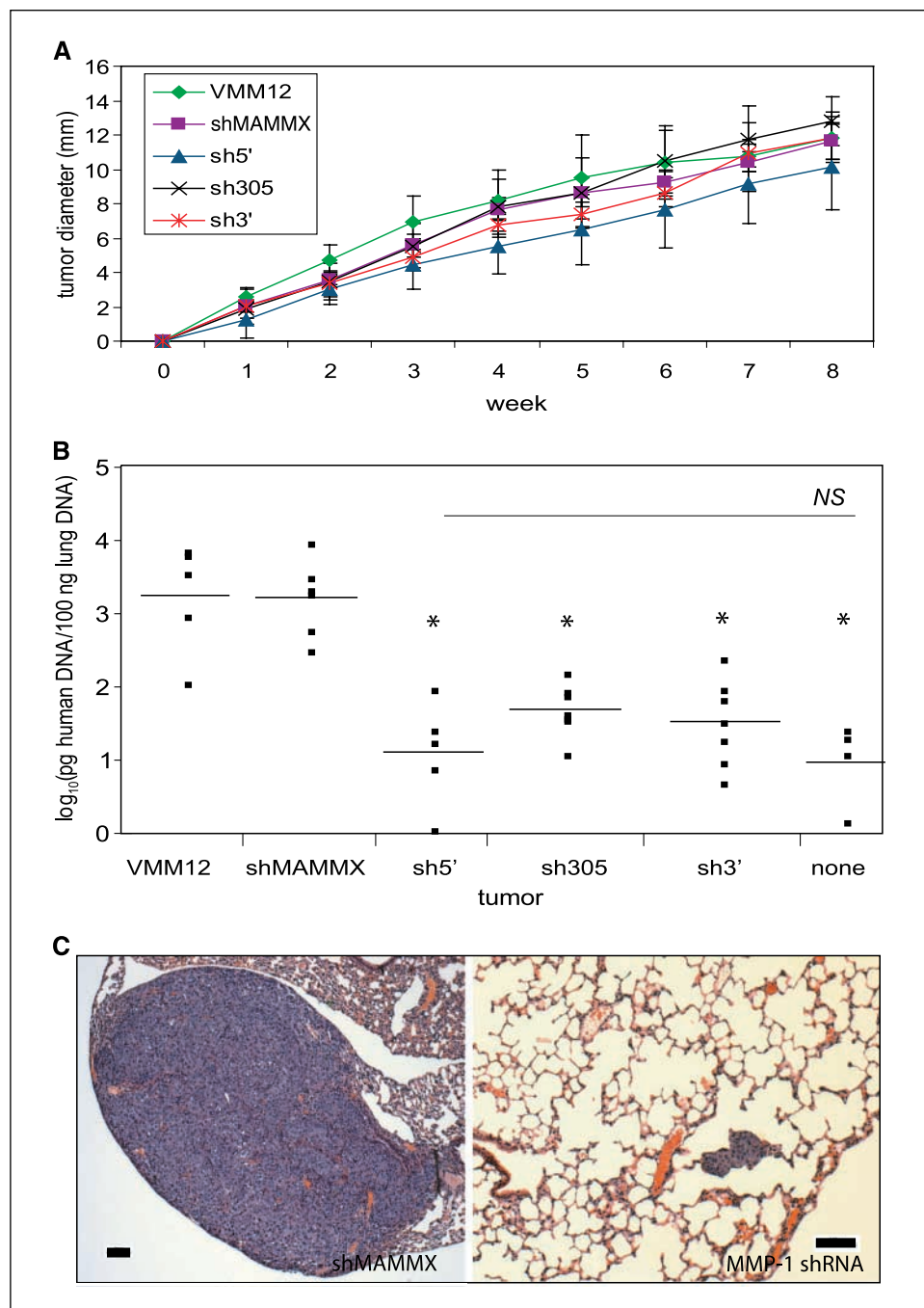


**Figure 2.** MMP-1 shRNA expression has no effect on melanoma tumor growth but significantly reduces metastatic burden. **A**, each cell line was injected interdermally into the right flank of nude mice at a density of  $5 \times 10^5$ . Tumors were measured weekly. Points, mean for each group; bars, SD. There was no difference in primary tumor growth between any of the shRNA cell lines and the VMM12 parental cell line. **B**, real-time PCR amplification of a human *AluI* sequence to quantify metastatic burden in the lung. The amount of human DNA in lung samples of mice injected with the different cell lines was quantitated and the results are presented as the log of pg human DNA per 100 ng lung DNA. Note that the Y axis is in log scale; thus, 0 is equivalent to 1 pg human DNA, 1 to 10 pg, 2 to 100 pg, etc. Each data point represents the mean value of three individual PCRs on the lung tissue from 1 mouse, and horizontal bars indicate the mean for each group. \*,  $P < 0.001$ , compared with shMAMMX control. NS, no significant difference between negative control and MMP-1 shRNA groups. **C**, H&E-stained sections showing a typical large metastatic tumor from a shMAMMX-injected mouse and a typical smaller metastasis from a MMP-1 shRNA-injected mouse. Bar, 100 μm.

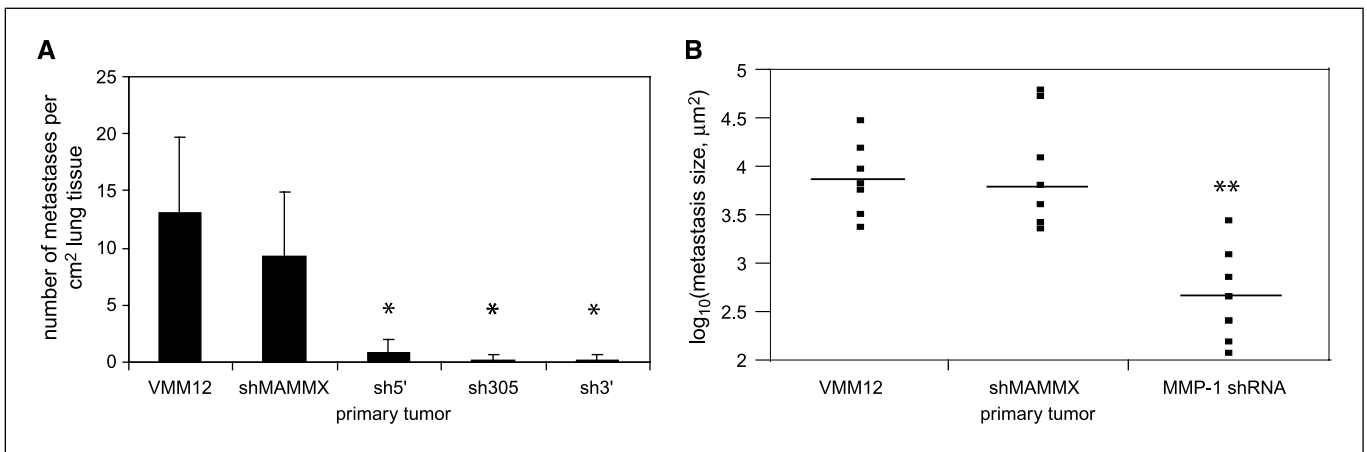


**Figure 3.** MMP-1 shRNA expression reduces both number and size of melanoma lung metastases. *A*, metastatic foci were counted in H&E-stained sections from the lung of each mouse and normalized to cm<sup>2</sup> lung tissue. Columns, mean number of foci for each group, with three sections analyzed per mouse; bars, SD. \*,  $P = 0.003$ , compared with shMAMMX control. *B*, the area, in µm<sup>2</sup>, for individual metastases was calculated for each group. Results are presented as the log of metastasis size, and each data point represents the size of one tumor. Note that the Y axis is in log scale. \*\*,  $P < 0.001$ , compared with shMAMMX control.

verify that MMP-1 is the primary MMP produced by VMM12 cells (10); they express 40- and 175-fold more MMP-1 than MT1-MMP and MMP-3, respectively, and the expression of other MMPs is negligible compared with MMP-1 (Fig. 1*A* and *C*). Expression of the shRNAs also did not change the proliferation rate of the cell lines (data not shown). Together, these data confirm the specificity of the shRNAs.

MMP-1 mediates the invasion of melanoma cells through type I collagen *in vitro* (21, 22), and this is largely attributed to the ability of MMP-1 to degrade the collagen surrounding the cells (27). To test the ability of each shRNA cell line to degrade type I collagen, cells were plated into an *in vitro* collagen destruction assay (24). The cells were mixed with 1 mL collagen and the mixture was allowed to gel. As the cells degraded the collagen, medium within the gel was released. With diminished MMP-1 expression, the three MMP-1 shRNA lines were unable to degrade the collagen gel, whereas the shMAMMX cells, expressing high levels of MMP-1, degraded almost all of the collagen, liberating ~0.8 mL of medium from the gel (Fig. 1*D*). These results show that MMP-1 shRNAs effectively block MMP-1 activity, whereas the control shRNA, MAMMX, has no effect on the collagenolytic ability of the melanoma cells.

**Stable knockdown of MMP-1 expression does not affect tumor growth but significantly decreases melanoma metastases.** To determine the function of MMP-1 in melanoma progression, the different cell lines were injected interdermally into nude mice. The rate of tumor growth was not significantly different among the cell lines (Fig. 2*A*), indicating that MMP-1 is not involved in tumor growth at the orthotopic site.

Mice were sacrificed when tumors reached ~12 mm in diameter. VMM12 tumors are highly metastatic to the lung (Supplementary Fig. S1*B*), and metastases were first quantified using real-time PCR to determine the amount of human DNA in 100 ng of total lung DNA from each mouse based on a protocol developed by Nicklas and Buel (26). shMAMMX-injected mice had, on average, 2,900 pg of human DNA per 100 ng of total lung DNA, whereas the sh5', sh305-, and sh3'-injected mice had an average of 30, 66, and 69 pg of human DNA in the lung, respectively ( $P < 0.001$ ; Fig. 2*B*). Additionally, the amount of human DNA in lungs of mice bearing MMP-1 shRNA primary tumors was not significantly

different than the nonspecific amplification that occurred when the PCR was run on lungs from naive mice, which had never been injected with melanoma cells ( $P = 0.16$ ). Again, this indicates that most of the mice injected with tumor cells harboring the MMP-1 shRNAs did not develop any metastatic tumors. These results show that diminished MMP-1 production by the primary tumor significantly decreases the capability of VMM12 melanoma cells to produce metastases.

The low amount of human DNA in the lungs of mice bearing MMP-1 shRNA tumors may be due to a decrease in the total number of metastases compared with shMAMMX-injected mice and/or due to a difference in the size of metastases between the groups. To differentiate between these possibilities, the lung tissue was examined. H&E-stained lung sections (Fig. 2*C*) showed that 100% of the shMAMMX-injected mice had melanoma metastases in their lungs, with an average of nine metastases per cm<sup>2</sup> lung tissue. In contrast, only 30% of mice injected with the MMP-1 shRNA cell lines had lung metastases, yielding an average of less than one tumor per cm<sup>2</sup> lung tissue (Fig. 3*A*). Further, MMP-1 shRNA metastases were significantly smaller than metastases from shMAMMX tumors ( $P < 0.001$ ; Figs. 2*C* and 3*B*). These data show that targeted knockdown of MMP-1 expression significantly decreases the ability of VMM12 melanoma cells to form metastases and may also inhibit the growth of the metastatic tumor.

**MMP-1 suppression affects the collagenase activity of the tumors.** Dermally invasive melanomas often express MMP-1, whereas noninvasive melanomas do not (18); a key component of the dermis is type I collagen, the major substrate for MMP-1. We (Fig. 1*D*) and others (22, 23) have shown that knockdown of MMP-1 expression in melanoma cells leads to a diminished capacity for collagen degradation and invasion *in vitro*. Because tumor cell invasion is directly related to collagenolytic activity (27), we postulated that the diminished capacity of the MMP-1 shRNA-expressing tumors to metastasize was related to their inability to degrade type I collagen *in vivo*.

In agreement with the *in vitro* data, tumors expressing the MMP-1 shRNAs had strong knockdown of MMP-1 expression compared with the shMAMMX tumors (Fig. 4*A*). To measure the ability of the tumors to degrade type I collagen, cross-sectional explants were taken from each tumor and used to condition serum-free medium

for 24 h. Medium collected from the MMP-1 shRNA tumor explants degraded significantly less collagen than medium from shMAMMX tumor explants ( $P < 0.001$ ; Fig. 4B). To determine the extent of MMP-1 involvement in the total collagenase activity of the tumor explants, conditioned media were next treated with a MMP-1 neutralizing antibody. When MMP-1 activity was thus blocked, collagenolytic activity in the shMAMMX tumor conditioned medium was greatly reduced (Fig. 4C). This indicates that MMP-1 is the main collagenase in the shMAMMX tumors and is responsible for the majority of the type I collagen degradation by these melanoma cells.

Together, these results show that MMP-1 is largely responsible for the ability of melanoma cells to degrade collagen and imply that MMP-1 is necessary for invasion of the dermal layer. Because

invasion is a vital step in melanoma progression, we propose that the diminished capability of the MMP-1 shRNA tumors to degrade type I collagen is directly related to the inability of the tumors to metastasize.

**MMP-1 shRNA expression reduces tumor-induced angiogenesis *in vivo*.** MMP production is essential for the formation of new blood vessels (28), and several MMPs have been definitively linked to tumor-induced angiogenesis, including MMP-2, MMP-9, and MT1-MMP (29). However, little data exist describing a role for MMP-1 in tumor-induced angiogenesis. In our *in vivo* experiment, blood vessels were more abundant along the tumor-bearing side of mice with shMAMMX tumors, and the tumors themselves were much more vascularized than tumors from mice injected with the

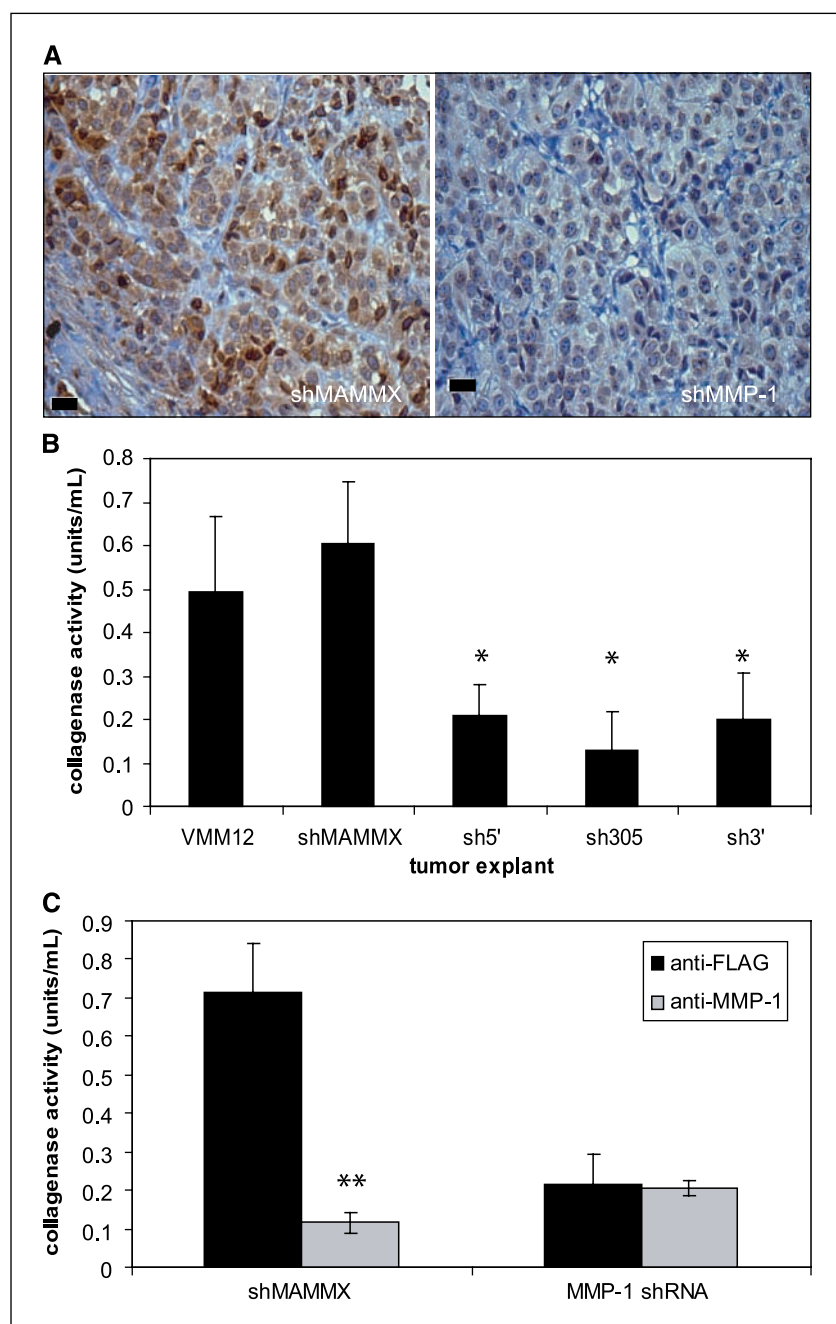


**Figure 4.** Suppression of MMP-1 expression *in vivo* results in significantly diminished collagenase activity. **A**, representative MMP-1 immunohistochemical staining of a shMAMMX tumor and a MMP-1 shRNA tumor. **Bar**, 20  $\mu$ m. **B**, explants were taken from each tumor during dissection and placed in serum-free medium for 24 h. The collagenase activity in the medium was then measured as described in Materials and Methods. **Columns**, mean of collagenase activity normalized to explant weight; tumor explants expressing the MMP-1 shRNA have impaired collagenolytic activity compared with the shMAMMX-expressing tumor explants. **Bars**, SD. \*,  $P < 0.001$ , compared with shMAMMX control. **C**, explant medium was treated with 1  $\mu$ g/mL of an anti-FLAG or a MMP-1 neutralizing antibody immediately before use in the assay. The MMP-1 neutralizing antibody significantly inhibited the collagenase activity of the shMAMMX tumor explants, indicating that MMP-1 is responsible for almost all of the collagenolytic activity of these cells. **Columns**, mean of collagenase activity normalized to explant weight, with results from the three MMP-1 shRNA groups averaged together; **bars**, SD. \*\*,  $P < 0.001$ , compared with anti-FLAG control.

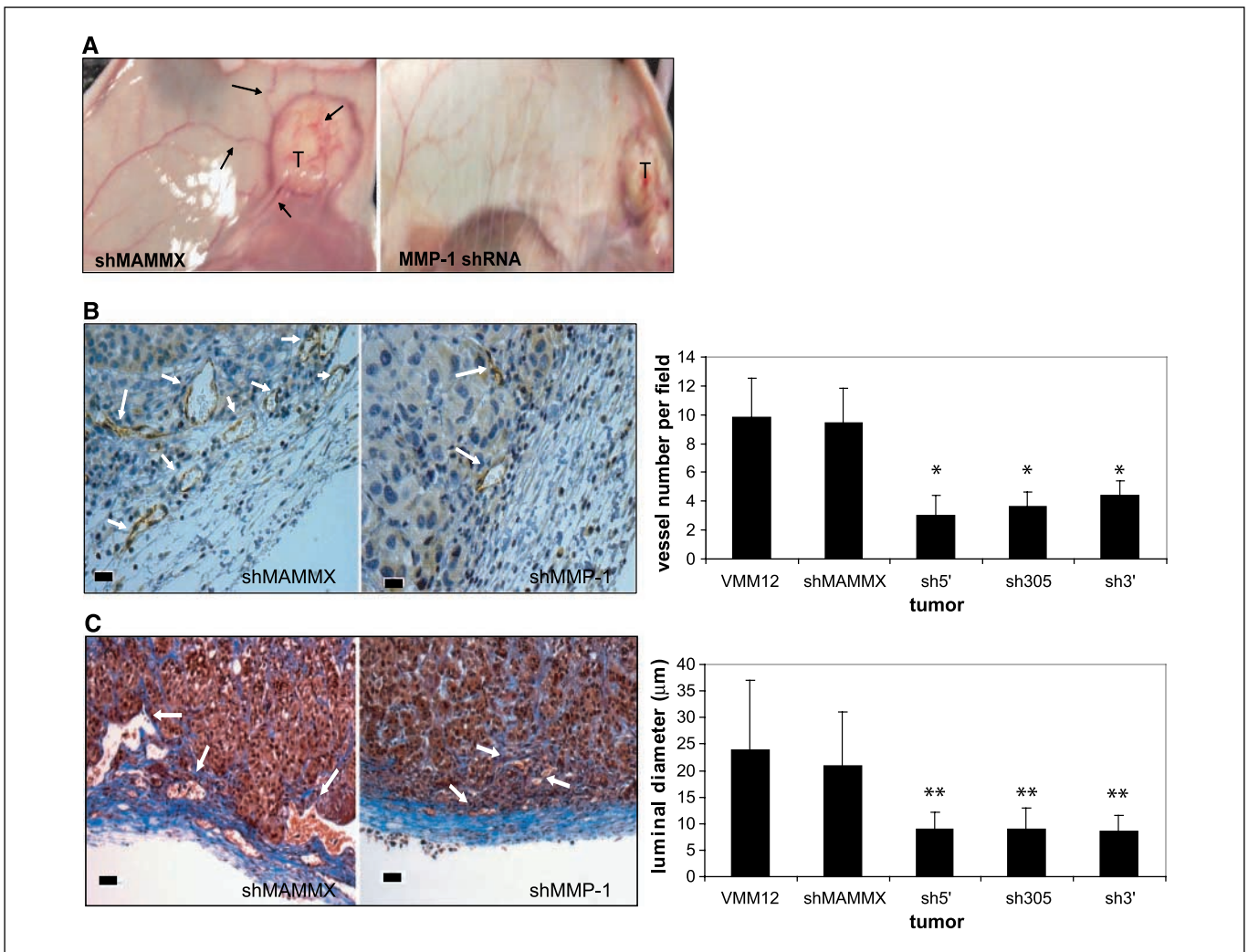


**Figure 5.** Attenuation of MMP-1 in melanoma tumors results in decreased angiogenesis. *A*, representative dissection photographs of shMAMMX and MMP-1 shRNA-injected mice. *Arrows*, increased vasculature in the shMAMMX mouse compared with the MMP-1 shRNA mouse. *B*, representative CD31 staining of shMAMMX and MMP-1 shRNA tumors. *Arrows*, CD31-positive blood vessels within each tumor. *Bar*, 20 µm. CD31-positive vessels were counted in three fields per tumor to determine the microvessel density. *Columns*, mean of the number of vessels per field and show that shMAMMX tumor tissue has approximately twice the number of blood vessels as the MMP-1 shRNA-expressing tumors; *bars*, SD. \*,  $P < 0.001$ , compared with shMAMMX control. *C*, representative Masson's trichrome staining of tumor sections used to highlight the luminal area of blood vessels (*arrows*) in the shMAMMX and the MMP-1 shRNA tumors. *Bar*, 50 µm. The smallest part of each lumen was measured for all blood vessels within a field, for three fields, and the results were averaged. *Columns*, mean of the luminal diameter in each tumor type; *bars*, SD. \*\*,  $P = 0.002$ , compared with control.

MMP-1 shRNA cell lines (Fig. 5A), indicating that MMP-1 may indeed contribute to angiogenesis.

To quantify these *in vivo* differences in angiogenesis, sections from each tumor were stained for endothelial cell-specific CD31 (Fig. 5B) and used for microvessel counts. There were ~10 CD31-positive vessels per field in shMAMMX tumor tissue, whereas only an average of 3.6 vessels per field were present in the MMP-1 shRNA tumors ( $P < 0.001$ ; Fig. 5B). Tumor tissue was next stained with Masson's trichrome to clearly define the luminal space in each vessel (Fig. 5C). A larger luminal area is indicative of a more mature vessel (30), and measurement of the luminal spaces showed that vessels within the shMAMMX tumors were approximately twice as large as the vessels within the MMP-1 shRNA tumors ( $P = 0.002$ ; Fig. 5C). These results show, for the first time, that MMP-1 expression by melanoma cells affects *in vivo* angiogenesis. Both microvessel density and vessel size have been correlated to melanoma metastasis (30), and it is therefore likely that the

significant decrease in both the size and number of blood vessels in the MMP-1 shRNA tumors is partly responsible for the decreased number of metastases in the MMP-1 shRNA tumor-bearing mice.

**MMP-1 enhances tube formation *in vitro*.** To determine the role of melanoma-produced MMP-1 in tumor-induced angiogenesis, the tube-forming ability of HMVECs was next examined. Tube formation by endothelial cells is a well-characterized *in vitro* measure of angiogenesis (31), as activated endothelial cells will differentiate to form a network of tube-like connections when plated on Matrigel, whereas inactive cells will not (Fig. 6A). Medium was conditioned by each melanoma cell line for 48 h and then added to HMVECs plated onto a thin layer of growth factor-reduced Matrigel. Conditioned medium from the shMAMMX cells induced many of the HMVECs to form tube-like structures, whereas HMVECs treated with conditioned medium from MMP-1 shRNA cell lines formed fewer tubes (Fig. 6A). Tube formation is typically quantified by branch point counting, as more branching

along the tubes is indicative of a more complex structure and, thus, a higher degree of *in vitro* angiogenesis (31). After several days in culture, highly complex, branched structures appeared in the wells treated with shMAMMX conditioned medium; in contrast, tubes formed by HMVECs treated with MMP-1 shRNA conditioned medium had very few branches (Fig. 6B). Overall, there was a significant decrease in the amount of branching by HMVECs stimulated with sh5', sh305, and sh3' conditioned medium compared with HMVECs treated with shMAMMX conditioned medium ( $P < 0.001$ ; Fig. 6C), indicating that MMP-1 induces activation of endothelial cells and promotes tube formation.

Recent studies showed that MMP-1 directly activates PAR-1 (32, 33). Activation of PAR-1 on endothelial cells causes intracellular calcium flux and von Willebrand factor release, hallmarks of endothelial cell activation (32, 33). We next sought to determine if the changes in branching between the HMVECs treated with either shMAMMX or MMP-1 shRNA conditioned medium were due specifically to MMP-1 in the medium and if the MMP-1/PAR-1 axis contributed to the tube-forming ability of the endothelial cells.

Inhibiting MMP-1 activity in shMAMMX conditioned medium using a MMP-1 neutralizing antibody blocked tube formation by the HMVECs, returning the number of branch points to levels similar to those seen using MMP-1 shRNA conditioned medium. Further, treating HMVECs with a specific PAR-1 antagonist, SCH79797, also significantly inhibited tube formation in the endothelial cells treated with shMAMMX conditioned medium ( $P < 0.001$ ; Fig. 6D). These results (a) show that melanoma-produced MMP-1 activates endothelial cells, likely via endothelial cell-expressed PAR-1, and promotes complex tube formation *in vitro* and (b) suggest that MMP-1 is playing a direct role in melanoma-induced angiogenesis.

## Discussion

Metastatic melanoma is an almost universally fatal disease, yet there have been few genes linked exclusively to the metastatic phenotype. More than 60% of all melanomas harbor an activating mutation in the Raf/MEK/ERK signaling pathway (34), and this has

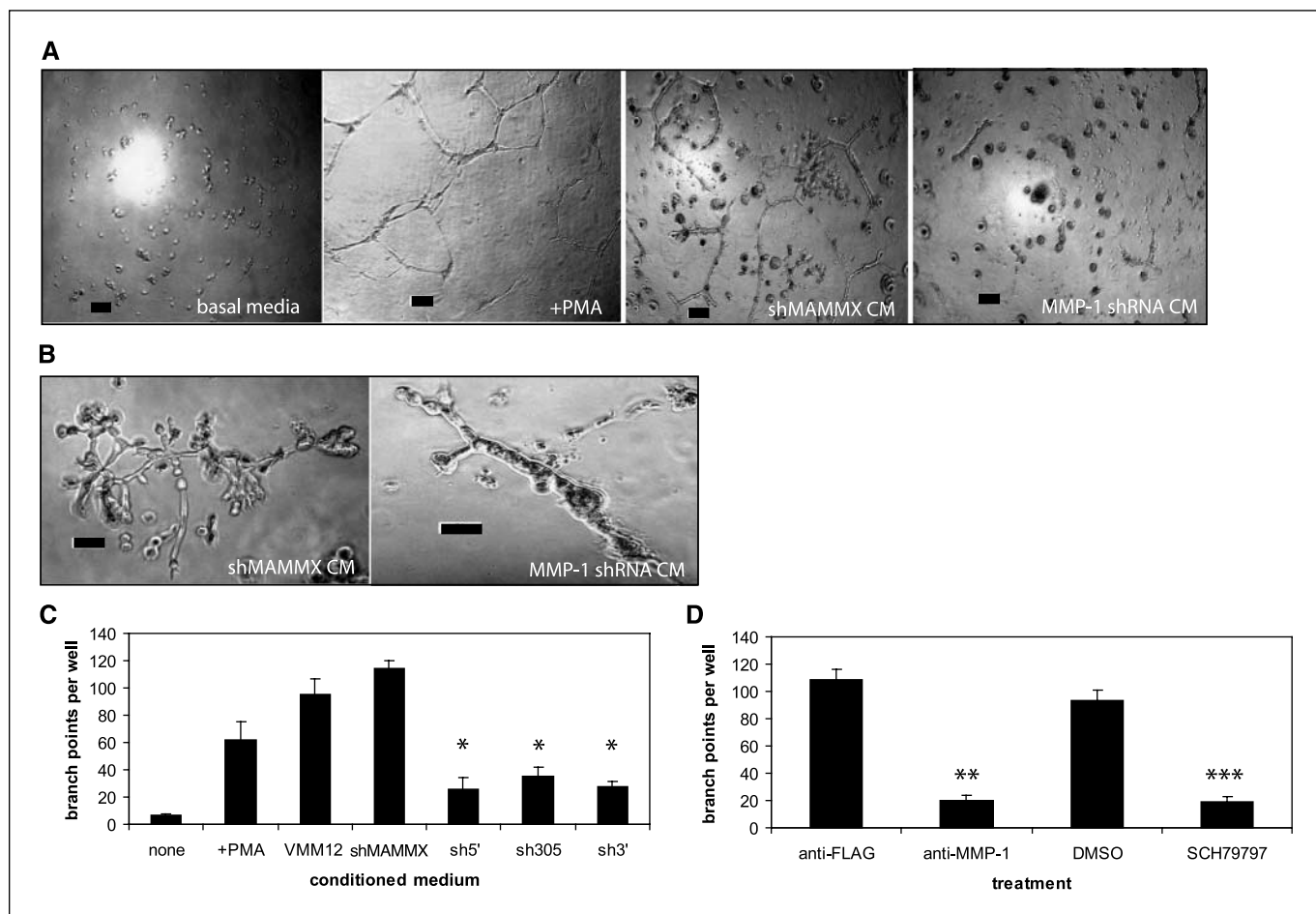


**Figure 6.** MMP-1 promotes the *in vitro* tube-forming ability of endothelial cells. **A**, representative micrographs of HMVECs plated in a tube formation assay as described in Materials and Methods. HMVECs were treated with basal medium alone (negative control), basal medium plus 50 ng/mL phorbol 12-myristate 13-acetate (PMA; positive control), HMVECs treated with basal medium conditioned by shMAMMX cells, and basal medium conditioned by MMP-1 shRNA cells. *Bar*, 100  $\mu$ m. **B**, higher-magnification representation of the complex branched structures found in wells treated with shMAMMX conditioned medium (CM) and the low level of complexity found in wells treated with MMP-1 shRNA conditioned medium. *Bar*, 50  $\mu$ m. **C**, quantification of the number of tube branch points per well. Treatment indicates either PMA addition to the medium (+PMA) or the cell line by which the medium was conditioned. *Columns*, mean number of branch points per well; *bars*, SD. \*,  $P < 0.001$ , compared with shMAMMX conditioned medium-treated wells. **D**, anti-FLAG and anti-MMP-1 neutralizing antibodies were added to shMAMMX conditioned medium immediately before use in the assay. HMVECs were treated with DMSO or the PAR-1 inhibitor SCH79797 before use in the assay. *Columns*, average number of branch points per well; *bars*, SD. \*\*,  $P < 0.001$ , compared with anti-FLAG-treated shMAMMX conditioned medium; \*\*\*,  $P < 0.001$ , compared with DMSO control.

been consistently associated with melanoma progression (4). However, the downstream effectors of ERK that are responsible for melanoma invasion and metastasis have not been previously defined. In the present study, we used shRNAs to specifically target a single gene, *MMP-1*, which is activated in the expansive Raf/MEK/ERK signaling cascade. Our results indicate that MMP-1 is not involved in primary tumor growth but is vital for the metastatic capability of VMM12 melanoma cells.

Of the four collagenases (MMP-1, MMP-3, MMP-8, and MT1-MMP), only MMP-1 has been consistently associated with a poor clinical outcome in melanoma (18, 35), indicating that MMP-1 is necessary for melanoma progression. MMP-1 localizes to dermally invasive melanoma cells (18, 36) and MMP-1-mediated invasion is directly related to the ability of the cells to degrade dermal type I collagen (27). In our studies, tumors with knocked down MMP-1 expression had significantly diminished collagenolytic activity and decreased metastatic potential compared with the control, suggesting a reduced invasive capability. These results agree with earlier clinical studies that correlate MMP-1 expression with high-grade invasive melanomas (18), linking the expression of the collagenase MMP-1 to progression from the epidermally confined RGP to the dermally invasive, metastatically competent VGP.

In melanoma, progression from benign tumor to malignant neoplasm requires the development of dynamic interactions between the tumor and the surrounding stromal environment (37), which includes tumor/endothelial cell interactions. Tumor-induced angiogenesis is required for growth of the primary tumor and is also a crucial step in the acquisition of a malignant phenotype (29).

Our data indicate that melanoma-produced MMP-1 is involved in tumor-induced vessel formation, as tumors with knocked down MMP-1 expression displayed obvious deficiencies in angiogenesis, both macroscopically and in size and number of capillaries within individual tumor sections (Fig. 5). Generally, primary tumors that are more heavily vascularized are more aggressive and have increased metastatic potential (38), and increased angiogenesis has been associated with the metastatic capability of melanoma (30). Interestingly, there was no significant change in primary tumor growth between MMP-1 shRNA and shMAMMX control tumors (Fig. 2), indicating that there was sufficient angiogenesis in both groups to sustain an equal growth rate. This may be attributed to the interdermal injection site, which is not well vascularized and causes tumors to grow relatively slowly, and to ulcerate and

become highly necrotic. There were, however, significant differences in the sizes of the metastatic tumors in the highly vascularized lung tissue (Fig. 3), and it is possible that the proangiogenic properties of MMP-1 have a greater effect on growth in these deep tissues. From these data, we conclude that the effect of MMP-1 on vessel formation directly contributes to the metastatic phenotype of VMM12 melanoma cells; increased angiogenesis provides a route of dissemination from the primary tumor and likely contributes to the growth of the metastatic tumor. This represents a novel role for MMP-1 in melanoma progression.

Because destruction of the ECM is necessary for vessel formation, considerable evidence has linked MMPs to tumor-induced angiogenesis (15, 29). Besides removing the physical barriers to new vessel growth, when MMPs proteolytically process components of the ECM, they release proangiogenic growth factors that are stored in the matrix, such as vascular endothelial growth factor, basic fibroblast growth factor, and platelet-derived growth factor (16, 29). Because MMP-1 is the major MMP produced by the VMM12 cell line (Fig. 1; ref. 10), we hypothesize that it is contributing to melanoma-induced angiogenesis in much the same way. Additionally, our data indicate that MMP-1 plays a direct role in tumor-induced angiogenesis, as MMP-1 is necessary to activate endothelial cells *in vitro* and induce tube formation. This direct cell-to-cell interaction adds to the repertoire of MMP-1 functions that are non-ECM related, and the MMP-1/PAR-1 axis seems to be central in this direct cross-talk between melanoma and endothelial cells.

In summary, our experiments show that, as a downstream effector of ERK signaling, MMP-1 enhances tumor cell collagenase activity and tumor-induced angiogenesis, which directly contributes to the metastatic capability of VMM12 melanoma cells. The Raf/MEK/ERK pathway is activated in a large proportion of melanomas, and because it is the uncontrollable metastatic spread of melanoma that is fatal, MMP-1 may be a therapeutic target in treating this disease.

## Acknowledgments

Received 5/16/2007; revised 9/7/2007; accepted 9/25/2007.

**Grant support:** NIH grants CA-77267 and AR-26599 (C.E. Brinckerhoff) and NIH grant T32-AI07363 (J.S. Blackburn).

The costs of publication of this article were defrayed in part by the payment of page charges. This article must therefore be hereby marked *advertisement* in accordance with 18 U.S.C. Section 1734 solely to indicate this fact.

## References

- Balch C, Soong S-J, Atkins M, Buzaid A, Thompson J. An evidence-based staging system for cutaneous melanoma. *CA Cancer J Clin* 2004;54:131-49.
- Leiter U, Friedegund M, Shittek B, Garbe C. The natural course of cutaneous melanoma. *J Surg Oncol* 2004;86:172-8.
- Gogas H, Kirkwood J, Sondak V. Chemotherapy for metastatic melanoma. *Cancer* 2007;109:455-64.
- Uribe P, Andrade L, Gonzalez S. Lack of association between BRAF mutation and MAPK ERK activation in melanocytic nevi. *J Invest Dermatol* 2006;126:161-6.
- Lopez-Bergami P, Huang C, Goydos J, et al. Rewired ERK-JNK signaling pathways in melanoma. *Cancer Cell* 2007;11:447-60.
- Jorgensen K, Holm R, Maelandsmo G, Florenes V. Expression of activated extracellular signal-regulated kinases 1/2 in malignant melanomas: relationship with clinical outcome. *Clin Cancer Res* 2003;9:5325-31.
- Satyamoorthy K, Li G, Gerrero M, et al. Constitutive MAPK activation in melanoma is mediated by both BRAF mutation and autocrine growth factor stimulation. *Cancer Res* 2003;63:756-9.
- Sharma A, Tran M, Liang S, et al. Targeting MAPK/ERK in the mutant (V600E) B-Raf signaling cascade effectively inhibits melanoma lung metastasis. *Cancer Res* 2006;66:8200-9.
- Kolch W, Kotwaliwale A, Vass K, Janosch P. The role of Raf kinases in malignant transformation. *Exp Rev Mol Med* 2002;25:1-18.
- Huntington JT, Shields JM, Der CJ, et al. Overexpression of collagenase 1 (MMP-1) is mediated by the ERK pathway in invasive melanoma cells. *J Bio Chem* 2004;279:33168-76.
- Park CH, Lee MJ, Ahn J, et al. Heat shock-induced matrix metalloproteinase (MMP)-1 and MMP-3 are mediated through ERK and JNK activation and via an autocrine interleukin-6 loop. *J Invest Dermatol* 2004;123:1012-9.
- Page-McCaw A, Ewald A, Werb Z. Matrix metalloproteinases and the regulation of tissue remodeling. *Nat Rev Mol Cell Biol* 2007;8:221-33.
- Stamenkovic I. Extracellular matrix remodelling: the role of matrix metalloproteinases. *J Pathol* 2003;200:448-64.
- Curran S, Murray GI. Matrix metalloproteinases: molecular aspects of their roles in tumour invasion and metastasis. *Eur J Cancer* 2000;36:1621-30.
- Yoon S-O, Park S-J, Yun C-H, Chung A-S. Roles of matrix metalloproteinases in tumor metastasis and angiogenesis. *J Biochem Mol Biol* 2003;36:128-37.
- Fingleton B. Matrix metalloproteinases: roles in cancer and metastasis. *Front Biosci* 2006;11:479-91.

17. Walker R, Wooley DE. Immunolocalisation studies of matrix metalloproteinases-1, -2 and -3 in human melanoma. *Virchows Arch* 1999;435:574-9.
18. Airola K, Karonen T, Vaalamo M, et al. Expression of collagenase-1 and -3 and their inhibitors TIMP-1 and -3 correlates with the level of invasion in malignant melanomas. *Br J Cancer* 1999;80:733-43.
19. Kurschat P, Wickenhauser C, Groth W, Krieg T, Mauch C. Identification of activated MMP-2 as the main gelatinolytic enzyme in malignant melanoma by *in situ* zymography. *J Pathol* 2002;197:179-87.
20. Hofmann U, Westphal J, Was E, et al. Matrix metalloproteinases in human melanoma cell lines and xenografts: increased expression of activated MMP-2 correlates with melanoma progression. *Br J Cancer* 1999; 81:774-82.
21. Benbow U, Schoenemark M, Mitchell T, et al. A novel host/tumor cell interaction activates matrix metalloproteinase 1 and mediates invasion through type I collagen. *J Bio Chem* 1999;274:25371-8.
22. Durko M, Navab R, Shibata H, Brodt P. Suppression of basement membrane type IV collagen degradation and cell invasion in human melanoma cells expressing an antisense RNA for MMP-1. *Biochim Biophys Acta* 1998;1356:271-80.
23. Iida J, McCarthy J. Expression of collagenase-1 (MMP-1) promotes melanoma growth through the generation of active transforming growth factor- $\beta$ . *Melanoma Res* 2007;17:205-13.
24. Wyatt CA, Geoghegan JC, Brinckerhoff CE. Short hairpin RNA-mediated inhibition of matrix metalloproteinase-1 in MDA-231 cells: effects on matrix destruction and tumor growth. *Cancer Res* 2005;65: 11101-8.
25. Meier F, Nesbit M, Hsu M, Martin B, Donatien P, Herlyn M. Human melanoma progression in skin reconstructs: biological significance of bFGF. *Am J Pathol* 2000;156:193-200.
26. Nicklas J, Buel E. Development of an Alu-based, real-time PCR method for quantitation of human DNA in forensic samples. *J Forensic Sci* 2003;48:1-9.
27. Ntayi C, Lorimier S, Berthier-Vergnes O, Hornebeck W, Bernard P. Cumulative influence of matrix metalloproteinase-1 and -2 in the migration of melanoma cells within three-dimensional type I collagen lattices. *Exp Cell Res* 2001;270:110-8.
28. Hass T, Madri J. Extracellular matrix driven matrix metalloproteinase production in endothelial cells. *Trends Cardiovasc Med* 1999;9:70-7.
29. Handsley M, Edwards D. Metalloproteinases and their inhibitors in tumor angiogenesis. *Int J Cancer* 2005; 115:849-60.
30. Demikese C, Buyukpinarbasili N, Ramazanoglu R, Oguz O, Mandel N, Kaner G. The correlation of angiogenesis with metastasis in primary cutaneous melanoma: a comparative analysis of microvessel density, expression of VEGF and bFGF. *Pathology* 2006; 38:132-7.
31. Staton C, Stibbling S, Tazzyman S, Hughes R, Brown N, Lewis C. Current methods for assaying angiogenesis *in vitro* and *in vivo*. *Int J Exp Pathol* 2004;85:223-48.
32. Boire A, Covic L, Agarvai A, Jacques S, Sherifi S, Kuliopulos A. PAR1 is a matrix metalloproteinase-1 receptor that promotes invasion and tumorigenesis of breast cancer cells. *Cell* 2005;120:303-13.
33. Goerge T, Barg A, Schnaeker E-M, et al. Tumor-derived matrix metalloproteinase-1 targets endothelial proteinase-activated receptor 1 promoting endothelial cell activation. *Cancer Res* 2006;66:7766-74.
34. Tuveson DA, Weber BL, Herlyn M. BRAF as a potential therapeutic target in human cancer. *Cancer Cell* 2003;4:95-8.
35. Nikkila J, Vihinen P, Vuoristo M-S, Kellokumpu-Lehtinen P, Kahari V-M, Pyrhonen S. High serum levels of matrix metalloproteinase-9 and matrix metalloproteinase-1 are associated with rapid progression in patients with metastatic melanoma. *Clin Cancer Res* 2005;11:5158-66.
36. Hofmann U, Westphal J, van Muijen G, Ruiter D. Matrix metalloproteinases in human melanoma. *J Invest Dermatol* 2000;115:337-44.
37. Smalley K, Lioni M, Herlyn M. Targeting the stromal fibroblasts: a novel approach to melanoma therapy. *Expert Rev Anticancer Ther* 2005;5:1069-78.
38. Pluda J. Tumor-associated angiogenesis: mechanisms, clinical implications and therapeutic strategies. *Semin Oncol* 1997;24:203-18.

# Cancer Research

The Journal of Cancer Research (1916–1930) | The American Journal of Cancer (1931–1940)

## RNA Interference Inhibition of Matrix Metalloproteinase-1 Prevents Melanoma Metastasis by Reducing Tumor Collagenase Activity and Angiogenesis

Jessica S. Blackburn, C. Harker Rhodes, Charles I. Coon, et al.

*Cancer Res* 2007;67:10849-10858.

<b>Updated version</b>	Access the most recent version of this article at: <a href="http://cancerres.aacrjournals.org/content/67/22/10849">http://cancerres.aacrjournals.org/content/67/22/10849</a>
<b>Supplementary Material</b>	Access the most recent supplemental material at: <a href="http://cancerres.aacrjournals.org/content/suppl/2007/11/09/67.22.10849.DC1">http://cancerres.aacrjournals.org/content/suppl/2007/11/09/67.22.10849.DC1</a>

<b>Cited articles</b>	This article cites 38 articles, 8 of which you can access for free at: <a href="http://cancerres.aacrjournals.org/content/67/22/10849.full#ref-list-1">http://cancerres.aacrjournals.org/content/67/22/10849.full#ref-list-1</a>
<b>Citing articles</b>	This article has been cited by 13 HighWire-hosted articles. Access the articles at: <a href="http://cancerres.aacrjournals.org/content/67/22/10849.full#related-urls">http://cancerres.aacrjournals.org/content/67/22/10849.full#related-urls</a>

<b>E-mail alerts</b>	<a href="#">Sign up to receive free email-alerts</a> related to this article or journal.
<b>Reprints and Subscriptions</b>	To order reprints of this article or to subscribe to the journal, contact the AACR Publications Department at <a href="mailto:pubs@aacr.org">pubs@aacr.org</a> .
<b>Permissions</b>	To request permission to re-use all or part of this article, use this link <a href="http://cancerres.aacrjournals.org/content/67/22/10849">http://cancerres.aacrjournals.org/content/67/22/10849</a> . Click on "Request Permissions" which will take you to the Copyright Clearance Center's (CCC) Rightslink site.